

Comparative Study on Calculation Methods of Temperature Field of Mass Concrete Structures in Subway Stations

Shuai Kou^{1,a}, Manlin Huo^{1*}, Lian Jin^{2,b}, Hua Nie^{3,c},
Yuxin Cao^{2,d}, Shaowei Ren^{1,e}, Chong Bian^{1,f}

^a826314638@qq.com; ^{*} huomlin@126.com; ^b361381292@qq.com; ^c181057853@qq.com;
^dkekexili2002@126.com; ^e2605957041@qq.com; ^f1693354128@qq.com.

¹School of Civil Engineering, Lanzhou Jiaotong University, Lanzhou 730070, China

²Sinohydro Railway Construction Co., Ltd., Beijing 1000703, China

³Sinohydro Bureau 7 Co., Ltd., Chengdu 611730, China

Abstract: When constructing the mass concrete temperature field, because the third type of boundary condition is difficult to deal with mathematically, the equivalent surface heat dissipation coefficient method or the equivalent thickness method is generally used for approximate processing in actual engineering. Based on different calculation methods, this study uses ABAQUS finite element software to establish three temperature field calculation models adds the concept of equivalent age, and compares and analyzes the error between the simulation results and the measured temperature. The calculation results show that after considering the equivalent age, the model of completely restoring the concrete surface insulation layer is the closest to the measured results, followed by the equivalent surface heat dissipation coefficient method; at the same time, both the simulation results and the measured results reflect that the concrete surface covering insulation materials can effectively control the temperature difference between inside and outside.

Keywords: mass concrete; temperature field; equivalent age; numerical simulation; ABAQUS

1 Introduction

The subway system is an important part of modern urban transportation. In recent years, in order to improve the level of urban infrastructure construction and public service capacity, the construction of subway stations has developed rapidly ^[1]. Due to the large volume and small specific surface area of the concrete roof, floor, and side wall of the subway station, the temperature of the concrete continues to rise after the completion of the pouring due to the influence of the cement hydration reaction, and the heat dissipation inside the concrete is slower than the surface. The temperature stress caused by the temperature difference between the inner and outer surfaces is easy to cause concrete cracking ^[2]. Because the concrete structure of the subway station is complex and the accuracy of the ordinary test is low in the underground environment, the researchers mostly use finite element software to simulate and analyze.

In the finite element software, ABAQUS is more mature in related fields [3]. Because ABAQUS software can not directly simulate the heat source over time but provides many user subroutine interfaces, these subroutines can make ABAQUS software more flexible and efficient in solving complex problems [4]. In this study, the subroutine HETVAL was used to edit it by FORTRAN language to realize the simulation of the mass concrete temperature field.

After the completion of the roof pouring, the upper surface concrete is directly exposed to the air, and its heat dissipation speed is faster than the lower surface, which will cause the overall cooling to be uncoordinated. In the project, the insulation material is usually covered for maintenance. Because the thermal parameters (such as density, thermal conductivity, specific heat, etc.) of concrete materials and insulation materials are quite different, in practical engineering, using the traditional heat conduction equation to estimate the thermal insulation effect of concrete surface insulation materials will produce large errors. Therefore, the equivalent surface heat dissipation coefficient method or the equivalent thickness method is generally used [5] However, these two methods are both simplified methods, and their accuracy is different from the actual situation. There is no relevant data for the calculation error between the two calculation methods and the complete reduction of the concrete insulation layer, and there are few papers for comparative analysis.

Based on the project of Chengdu Metro Line 19 Terminal 2, this study uses ABAQUS numerical simulation software to simulate the temperature field of the concrete roof of the subway station. Through different boundary condition treatment methods, a reasonable numerical model is established to simulate the temperature change of the concrete roof of the subway station, which provides a scientific basis and guidance for exploring the influence of mass concrete temperature field on its mechanical properties and the design and construction of subway station buildings.

2 Relying on the project overview

Shuangliu Airport Terminal 2 (formerly Shuangliu Airport Station) is located in the ground parking lot in front of Shuangliu International Airport Terminal 2. It is arranged in the north-south direction parallel to the South Second Road of the airport. It is an island platform station with three floors, two spans, and 12 m underground. The total length of the station is 696.2 m, and the buried depth of the foundation pit is 26.59 m, which is constructed by open excavation.

In this study, the concrete roof of the negative first floor of section 9 of the station (Figure 1.) was selected as the research object. The thickness of the roof was 0.9 m × 1.2 m, the two spans were 21.9 m in total, and the size of the beams on both sides was 0.8 m × 2 m. The size of the middle stringer is 1.2 m × 2.1 m, and the length of the construction section is 24.8 m. The roof and beam are poured together, and the pouring date is in May. The supporting template was 2 cm plywood, which was removed after 14 days. The upper surface was covered with plastic film and 3 mm geotextile, which was removed after 7 days of curing.

The strength grade of roof and beam concrete is C35, $\rho_0=2450 \text{ kg/m}^3$; the cement adopts P·O 42.5 grade, which is produced by Sichuan Desheng Group Cement Co., Ltd.; the fly ash is supplied by Guang 'an Xinyuan Environmental Protection and Energy-saving Building Materials Co., Ltd., with a dosage of 20 %.

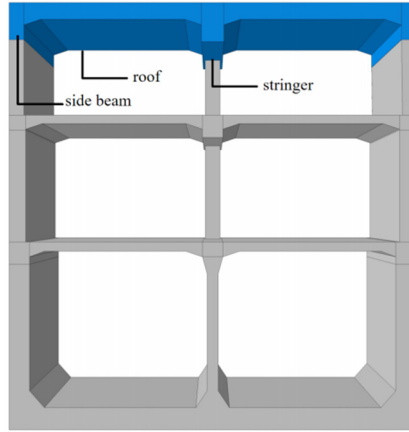


Figure 1. Structure diagram of the subway station

3 Calculation principle and calculation data of hydration heat temperature field

3.1 Boundary conditions of temperature field

In the thermal analysis of concrete, the boundary condition is to reflect the heat exchange relationship between the concrete surface and the surrounding medium [6]. According to the function relationship of concrete surface temperature changing with time, the boundary conditions can be divided into four categories [7]:

(1) The temperature T of the concrete surface is a known function of time:

$$T(\tau) = f(\tau) \quad (1)$$

(2) The heat flux of concrete surface is a known function of time:

$$-\lambda \frac{\partial T}{\partial n} = f(\tau) \quad (2)$$

In the formula: n is the normal direction of the outer surface of the concrete structure; when the surface is adiabatic, $\frac{\partial T}{\partial n} = 0$.

(3) When the surface of the concrete is in contact with the outside air is a convective heat transfer boundary :

$$-\lambda \frac{\partial T}{\partial n} = \beta(T - T_a) \quad (3)$$

In the formula: β is the convective heat transfer coefficient; T_a is the external temperature.

(4) When the concrete slab and the solid contact, if the contact surface temperature and heat flow are continuous, the boundary conditions are :

$$T_1 = T_2, \lambda_1 \frac{\partial T_1}{\partial n} = \lambda_2 \frac{\partial T_2}{\partial n} \quad (4)$$

3.2 Calculating data

3.2.1 Adiabatic temperature rise equation

In all adiabatic temperature rise models describing concrete, the composite exponential formula is more accurate^[8] that is:

$$Q(\tau) = Q_0(1 - e^{-a\tau^b}) \quad (5)$$

In the formula: Q_τ —Cumulative heat release of concrete at age τ ,kJ/kg;

τ —age ,d;

Q_0 —Total hydration heat of concrete,kJ/kg;

a and b are constants, which are 0.69 and 0.56 respectively.

3.2.2 Calculation of concrete hydration heat

(1)Cement heat release

The total hydration heat Q_0 of cement is determined according to reference [9], select $Q_0=330$ kJ/kg^[9].

(2)Heat release of cementitious materials

According to the specification [10], the total amount of hydration heat Q of cementitious materials is calculated according to Formula(6)^[10]:

$$Q = kQ_0 \quad (6)$$

In the formula: k —adjustment facto.

Table 1. Hydration heat adjustment coefficient of fly ash with different content

Coal ash percentage	0	10%	20%	30%	40%
k	1	0.96	0.95	0.93	0.82

Note: The content in the table is the percentage of fly ash in the total amount of cementitious materials. Table 1, $k = 0.95$, the total hydration heat Q of cementitious material is:

$$Q=kQ_0=0.95 \times 330=313.5 \text{ kJ/kg}$$

3.2.3 Calculation of thermal parameters of concrete

In the calculation of concrete temperature field, thermal conductivity λ and specific heat c are basic physical parameters, which directly affect the heat transfer characteristics of concrete. In this study, the λ and c of concrete are obtained by the weight percentage weighting method according to the coefficients provided by the literature and the specification (see Table 2)^[9]-^[11]. The λ and c of fly ash are selected according to cement parameters.

Table 2. Mix proportion and thermal performance coefficient of concrete materials

Project	Unit	Water	Cement	Flyash	Sand	Pebble	Water reducing agent	Waterpro of agent
Weight	kg	170	330	83	787	1023	7.43	29.00
Percentage	%	7.00	13.58	3.42	32.39	42.11	0.31	1.19
Thermal conductivity	$\text{kJ}/(\text{m}\cdot\text{h}\cdot^\circ\text{C})$	2.16	4.59	4.59	11.10	14.19	—	—
Specific heat	$\text{kJ}/(\text{kg}\cdot^\circ\text{C})$	4.19	0.54	0.54	0.75	0.76	—	—

Thermal conductivity:

$$\lambda = 1.05 \times (7.00 \times 2.16 + 17.00 \times 4.59 + 32.39 \times 11.10 + 42.11 \times 14.19) / 100 = 11.029 \text{ kJ} / (\text{m} \cdot \text{h} \cdot ^\circ\text{C})$$

Specific heat:

$$c = 7.00 \times 4.19 + 17.00 \times 0.46 + 32.39 \times 0.75 + 42.11 \times 0.76 / 100 = 0.945 \text{ kJ} / (\text{kg} \cdot ^\circ\text{C})$$

3.3 Method of calculation

When calculating the temperature field of concrete, the third boundary condition is usually approximated by the equivalent surface heat dissipation coefficient method or the equivalent thickness method.

3.3.1 Equivalent surface coefficient of the heat transfer method

When the concrete surface is attached to thermal insulation material, it is necessary to select the heat dissipation coefficient β to consider the influence of the thermal insulation layer.

The calculation formula of the equivalent surface heat dissipation coefficient β_s is shown in Formula (7)^[9]:

$$\beta_s = \frac{1}{R_s} = \frac{1}{(1/\beta) + \sum (h_i / \lambda_i)} \quad (7)$$

In the formula: R_s —Total thermal resistance of insulation layer, $(\text{m}^2 \cdot \text{h} \cdot ^\circ\text{C})/\text{kJ}$;

β —The heat dissipation coefficient of the outermost insulation layer in the air, $\text{kJ}/(\text{m}^2 \cdot \text{h} \cdot ^\circ\text{C})$;

h_i —Insulating layer thickness, m;

λ_i —Thermal conductivity of insulation layer, $\text{kJ}/(\text{m} \cdot \text{h} \cdot ^\circ\text{C})$.

Due to the different material and thickness of the thermal insulation layer around the roof, the surface β_s is different. The material parameters of the thermal insulation layer are shown in Table 3.^[9-10,13]; Among them, the upper surface of the roof is covered with plastic film and geotextile maintenance, but the thickness of the plastic film is only 0.01 mm, and the thermal insulation effect can be ignored. Although the subway station is constructed by open excavation, the influence of wind speed is not considered because it is underground.

Table 3. Parameters of each insulation layer

Thermal insulating material Design conditions	Geotextiles	Veneer plywood
Thickness h /m	0.003	0.02
Density ρ /kg·m ⁻³	300	600
Thermal conductivity λ /kJ·(m·h·°C) ⁻¹	0.144	0.612
Specific heat c /kJ/(kg·°C)	1.630	2.510
Surface coefficient of heat-transfer β /kJ·(m ² ·h·°C)	21.06	18.46

Substituting table 3 parameters into formula (7), β_s of surface of concrete can be calculated, as shown in table 4.

Table 4. The equivalent surface heat dissipation coefficient of each insulation layer

	The upper surface of the roof	The lower surface of the roof	Side of the roof
Equivalent surface coefficient β_s kJ/(m ² ·h·°C)	14.638	11.514	11.514

Note : The section connected to the old concrete is taken as the adiabatic surface.

3.3.2 Equivalent thickness method

The equivalent thickness method is to extend a virtual boundary from the real boundary to form a virtual equivalent thickness, thereby simplifying the heat conduction calculation. According to Formula (3), if the concrete surface is covered with insulation layer, the temperature T at the boundary is [12]:

$$\lambda_i \frac{\partial T}{\partial n} + \beta_s (T - T_a) = 0 \quad (8)$$

In the formula: λ_i —Thermal conductivity of insulation layer ,kJ/(m·h·°C);

T —Surface temperature of concrete ,°C;

n —Outer normal direction of surface boundary;

β_s —Equivalent surface heat dissipation coefficient of insulation layer ,kJ/(m²·h·°C);

T_a —Ambient temperature ,°C.

The equivalent thickness is the distance between the virtual boundary and the real boundary, which is $d = \lambda / \beta_s$. The heat exchange between the virtual boundary and the outside world can be regarded as infinite, so the surface temperature of the virtual boundary is the same as the ambient temperature. From this, the surface d of concrete can be calculated, as shown in Table 5.

Table 5. The equivalent thickness of each insulation layer

	The upper surface of the roof	The lower surface of the roof	Side of the roof
Equivalent thickness d /m	0.75	0.96	0.96

Note : The section connected to the old concrete is taken as the adiabatic surface.

3.4 Equivalent age maturity

The essence of heat release from cement hydration is the chemical reaction of cement hydration^[14]. The hydration reaction of cement will lead to the increase of concrete temperature, which will accelerate the hydration rate of cement^[15]. Therefore, the equivalent time and the degree of hydration are combined to simulate the temperature field of early concrete more accurately.

According to the Arrhenius equation, Hansen et al^[16] proposed a new characterization method of maturity theory, and the equivalent age t_e is:

$$t_e = \int_0^t \exp \frac{E_A}{R} \left(\frac{1}{T_r} - \frac{1}{T} \right) dt \quad (9)$$

In the formula: E_A —Reaction activation energy, J/mol;

R —Ideal gas constant, 8.314 J/(mol·K);

T_r —Reference temperature (Usually take 20 °C, is 293 K);

T —The actual absolute temperature of the node.

In the finite element simulation calculation, the corresponding equivalent age value is calculated by the cumulative superposition of time steps. When the absolute temperature $T \geq 293$ K, $E_A = 33.5$ kJ·mol⁻¹; When $T < 293$ K, $E_A = 33.5 + 1.47 \times (293 - T)$ (kJ·mol⁻¹)^[17]. Within 15 days after pouring, $E_A/R = 2700$ K was selected^[18].

3.5 HETVAL subroutine

In the analysis of the concrete temperature field, the heat generated by cement hydration heat is a heat source that changes with time^[19]. This study uses the HETVAL subroutine to achieve this heat source function.

The main part of the HETVAL program is shown below :

```
SUBROUTINE
HETVAL(CMNAME,TEMP,TIME,DTIME,STATEV,FLUX,PREDEF,DPRED)
INCLUDE 'ABA_PARAM.INC'
CHARACTER*80 CMNAME
usercoding to define FLUX and update STATEV
DIMENSION TEMP(N),STATEV(N),PREDEF(*),TIME(N),FLUX(N),DPRED(*)
END
```

Among them: CMNAME is the material name; TEMP is the temperature array at the current time step; TIME is the time array under the current time step; DTIME is the time step; STATEV is the material state variable; FLUX is the material heat source in the current time step; PREDEF is an array containing all custom field variables; DPRED is an incremental array of predefined field variables.

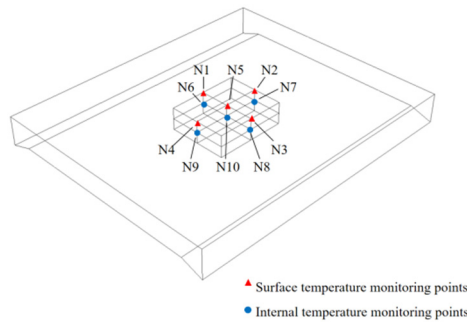
4 Finite element simulation

According to the above calculation data, the finite element model of the station roof is established by using the finite element software ABAQUS, and compared with the measured temperature.

4.1 Layout of monitoring points and measured temperature fitting

4.1.1 Layout of monitoring points

Due to the long pouring time of concrete, the cementitious material has been heated up by hydration heat release during the pouring process, but the temperature rise process is not stable due to the influence of environment, construction, and other factors. Therefore, 2 h after pouring is taken as the starting point of the measured temperature, and the measurement time is 168 h. The JDC-2 building electronic thermometer was used, and the N1-N10 at the roof was selected as the monitoring point, as shown in Figure 2.



(a) Temperature measuring point layout



(b) Temperature measuring instrument

Figure 2. Temperature measuring point layout and temperature measuring instrument

4.1.2 Measured temperature fitting

Fit the measured temperature data, as shown in Fig 3

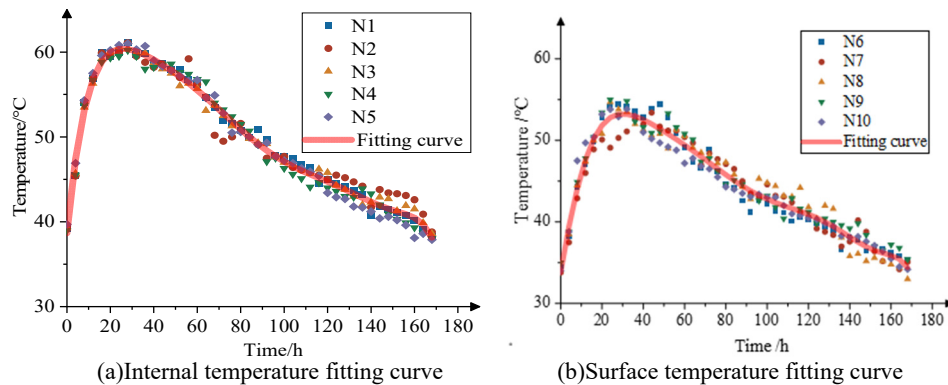


Figure 3. Concrete temperature fitting curve

The internal temperature fitting degree of concrete is $R^2 = 0.983$, and the surface temperature fitting degree of concrete is $R^2 = 0.959$, which meets the accuracy requirements.

4.2 Ambient temperature data

According to statistics, the local temperature is shown in Fig.4.

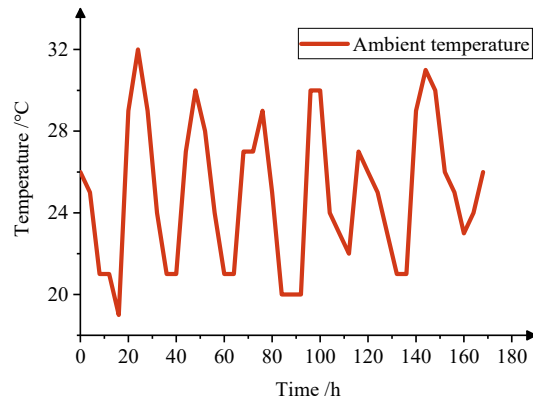


Figure 4. Ambient temperature

4.3 Establishment of concrete roof model

According to different calculation methods, three finite element models are established, as shown in Fig.5. Model 1 completely restores the insulation layer of the concrete boundary ; model 2 adopts the equivalent surface heat dissipation coefficient method ; model 3 adopts the equivalent thickness method.

The transient analysis of heat transfer was selected in the analysis step, and the time was 170 h. In the predefined field, the initial temperature of concrete is 28 °C, and the DC3D8 eight-node linear heat transfer hexahedral unit is used. Because the temperature is measured 2 hours after the completion of the field pouring, the time coordinate of the simulation is selected 2 hours as 0 scale to start statistics. The difference is that the surface of the model 1 is set as the surface heat exchange condition in the interaction module, and the heat dissipation coefficient is selected according to table 3. The surface of the model 2 is set as the surface heat exchange condition in the interaction module, and the heat dissipation coefficient is selected according to table 4. Model 3 selects temperature boundary conditions in the load module.

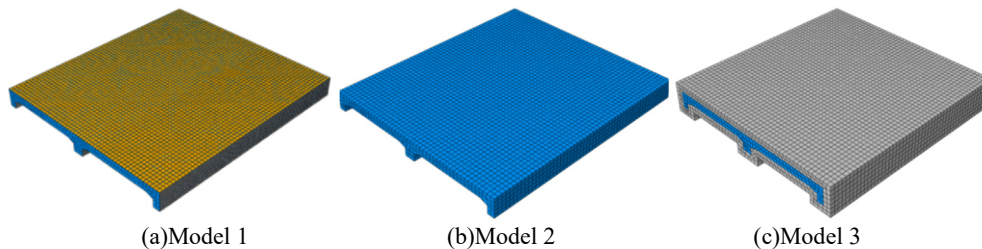


Figure 5. Concrete roof model

4.4 Total heat release and heat release rate

Because the concrete property parameters of the three models are consistent, and the temperature changes are relatively close, the total heat release and the heat release rate are not much different, so only one group needs to be displayed. The simulation results are shown in Fig.6.

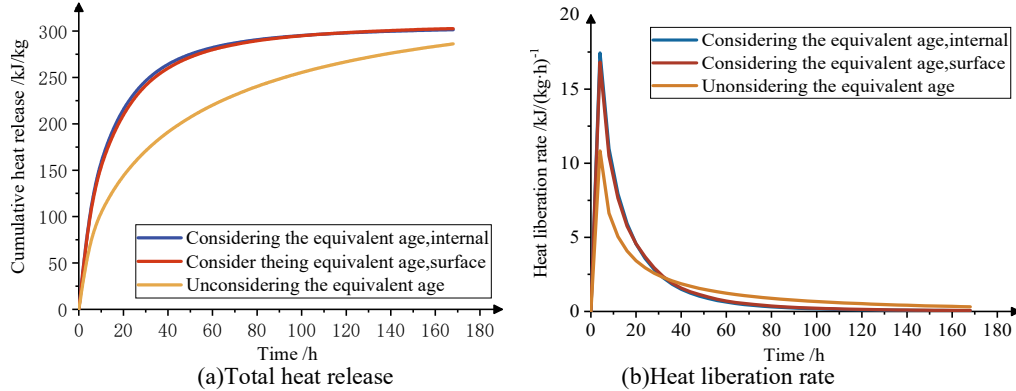


Figure 6. Model 1 Total heat release and heat release rate of concrete

4.5 Simulation results of concrete roof temperature

The temperature calculation results and temperature distribution nephogram of the three models are shown in Fig 7 to 12.

(1) Model 1

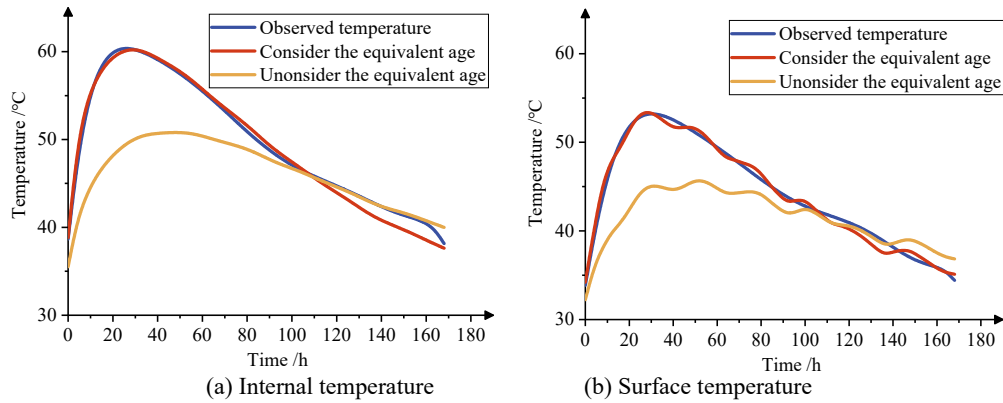


Figure 7. Model 1 concrete temperature calculation results

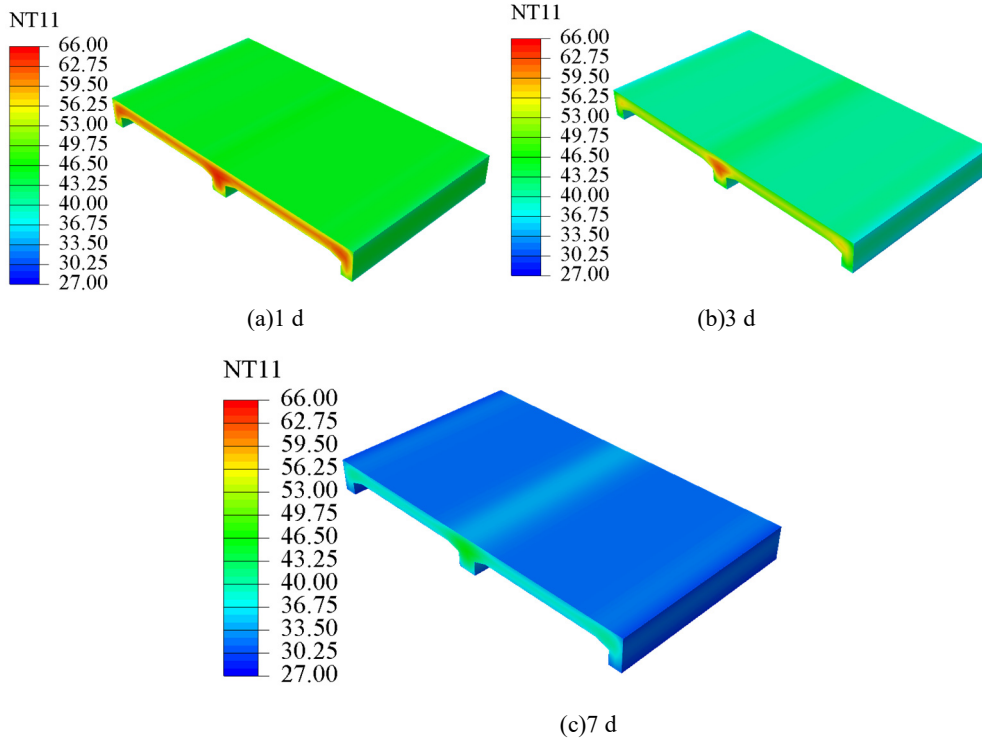


Figure 8. Model 1 7 d temperature distribution cloud map

(2) Model 2

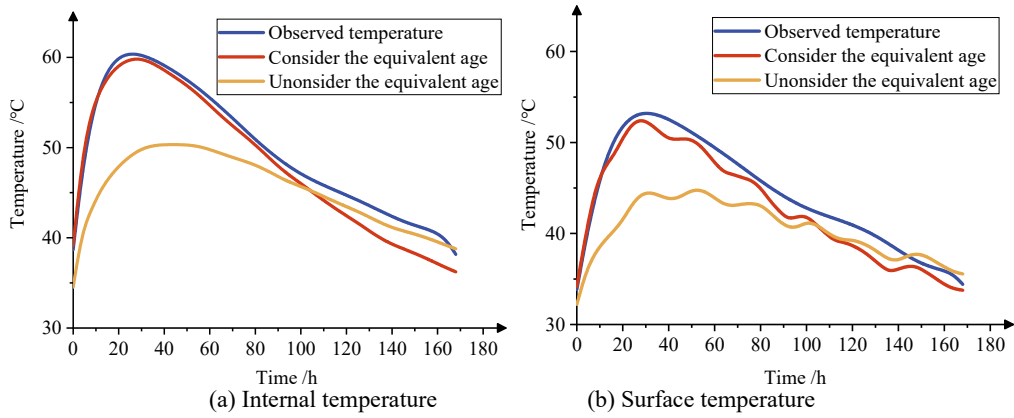


Figure 9. Model 2 concrete temperature calculation results

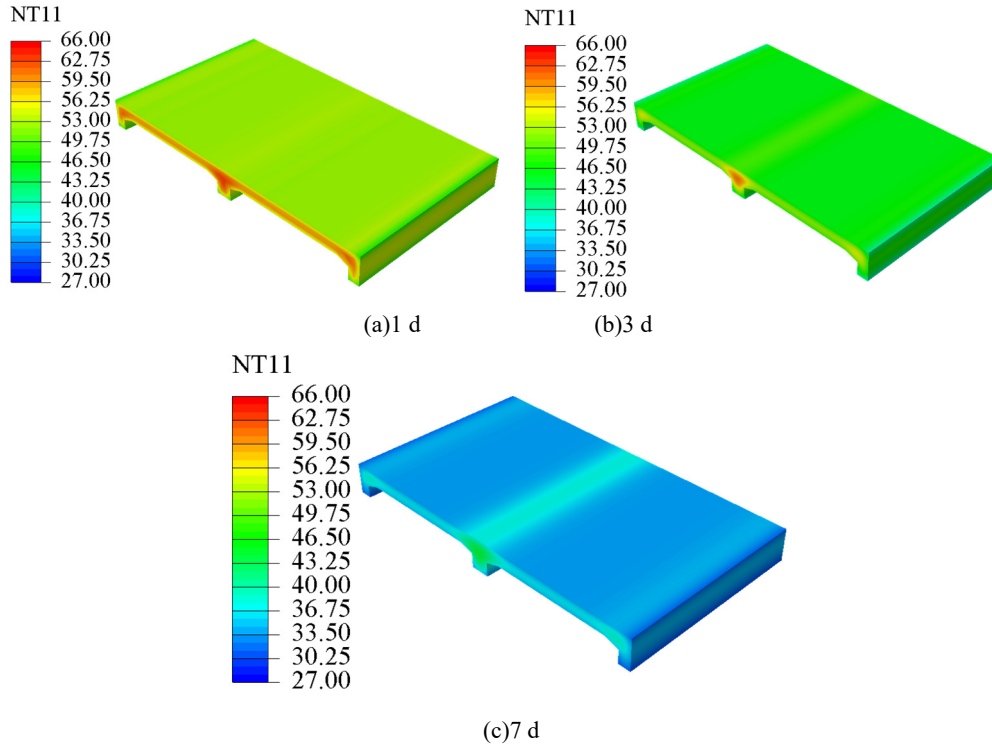


Figure 10. Model 2 7 d temperature distribution cloud map

(3) Model 3

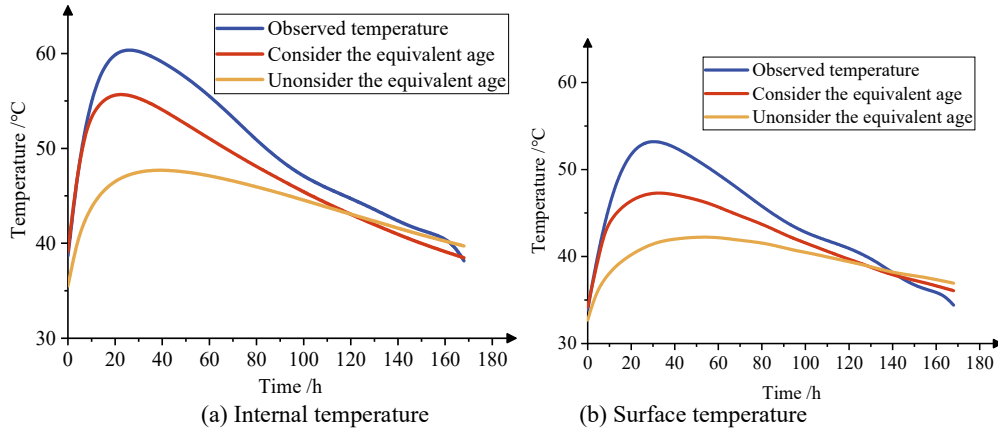


Figure 11. Model 3 concrete temperature calculation results

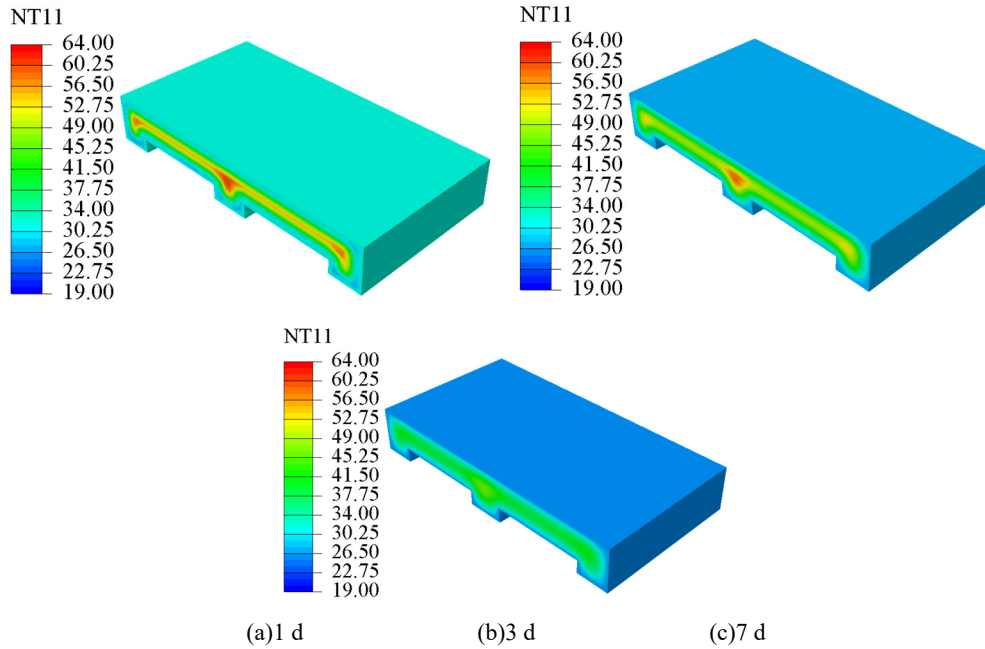


Figure 12. Model 3 7 d temperature distribution cloud map

4.6 Simulation error

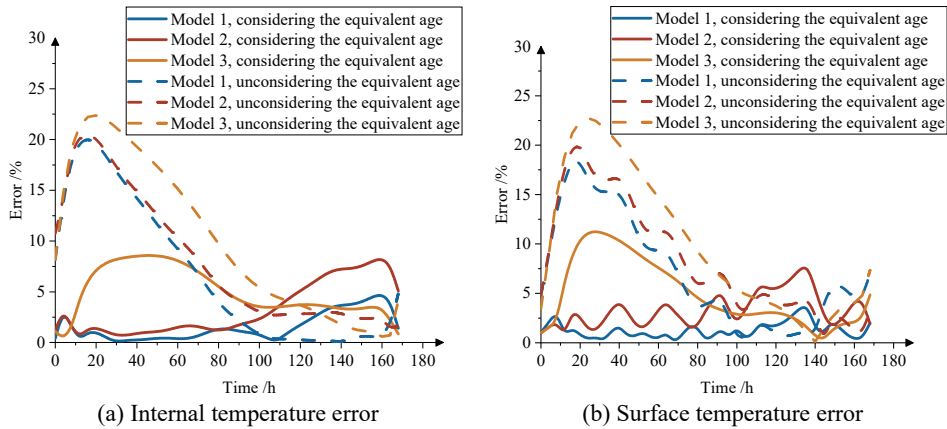


Figure 13. Statistics of internal and external temperature error of concrete

5 Conclusion

(1) According to the error results (as shown in Fig 13), in the simulation of concrete internal temperature, considering the equivalent age, the average errors of the three models are 1.54 %, 3.25 % and 4.96 % respectively. Without considering the equivalent age, the average errors of

the three models are 6.73 %, 8.14 % and 10.11 % respectively. In the simulation of concrete surface temperature, considering the equivalent age, the average errors of the three models are 1.27 %, 3.35 % and 4.97 % respectively. Without considering the equivalent age, the average errors of the three models are 7.11 %, 8.33 % and 10.01 % respectively.

From the above, it can be seen that in the case of considering the equivalent age, the model 1 (completely reduced concrete insulation layer) has the smallest error, but the modeling process is more complicated ; the error of model 2 (equivalent surface heat dissipation coefficient method) is second, but the modeling process is relatively simple. It only needs to establish the main structure of concrete, which can reduce the number of elements and ensure the calculation accuracy. The error of model 3 (equivalent thickness method) is large. Because of the large thickness and many division units, the calculation amount is large.

(2) According to the data analysis of Model 1, the maximum temperature of the center of the concrete roof is 60.3 °C, and the maximum temperature of the surface is 52.8 °C, both of which appear at 30 h after pouring. The maximum temperature difference of the inner surface is 9.55 °C, which appears in the 18 h after pouring.

(3) Both the simulation results and the measured results show that after covering the surface of the concrete roof of the station with thermal insulation materials, the maximum temperature difference between the inside and the surface is controlled within 10 °C, which meets the requirements of mass concrete construction standards.

(4) The hydration heat release rate of concrete reaches the peak in the early stage. Considering the equivalent age, the hydration heat of concrete reaches 90 % of the total amount at 60 h and 96.6 % at 168 h. Without considering the equivalent age, the hydration heat of concrete reaches 90 % of the total amount at 156 h and 91.7 % at 168 h.

References

- [1] Wang R, Lu T Y, Cheng K.(2023) Study on Application Standardization of Construction Information Model for Subway Stations. *Modern Tunnelling Technology*, 60(1): 47-55. DOI:10.13807/j.cnki.mtt.2023.01.005.
- [2] Zhu Z Y.(2020) Temperature field calculation of mass concrete structure.China Water&Power Press, BeiJing. www.waterpub.com.cn
- [3] Luo C.(2020) Research on temperature field of continuous reinforced concrete pavement and sensitivity analysis of design parameters. *Journal of China & Foreign Highway*, 40(03):76-80.DOI:10.14048/j.issn.1671-2579.2020.03.016.
- [4] Wang Q, Huo Y W, Xia F, Liu B, Xiang H, Wang S D, Hao Z H, Gao X.(2015) Mass concrete hydration heat temperature field of numerical analysis based on ABAQUS. *Concrete*,(07):35-39+48. Doi: 10.3969/j.issn.1002-3550.2015.07.009
- [5] Zhao L J.(2008) Research on calculation method about superficial heat preservation of massive concrete. Xi'an University of Technology, Xi'an.https://kns.cnki.net/kcms2/article/abstract?v=2F6201taHdeCsuUF-m3N4SPqn9kbyPIMFCPSu1StIDh_n-GigaRxJGgqMm031tc43wHP5xkhOeWkG9svYgIwj9FOca_dQoWPM_SaU4utNiIApB8vEnpBlinS OtnnAt5p&uniplatform=NZKPT&language=CHS

- [6] Ren X, Qi Y, W L etc.(2022) Research on thermal actions of concrete thin-walled pylon structure with or without thermal insulation measures [J]. Concrete.No.391(05):48-51+56. Doi:10.3969/j.issn.1002-3550.2022.05.010
- [7] Men F.(2022) Study on crack resistance of concrete long beam under temperature stress. Chang'an University, Xi'an. https://kns.cnki.net/kcms2/article/abstract?v=2F6201taHdc14yHwP4HopK6s8fiJD7sGM3bEnOjbt2aBnfreTP2dfM_Oyv2hvHd4MPyFSa_MvFUNcUaqhF6lZ6JPBg8LvTutS4v08NXpFjRLgp5f86x27eYxWuN12UjCan-Bezsh2YOSybl2d6Qg==&uniplatform=NZKPT&language=CHS
- [8] Zhu B F.(2011) Compound exponential formula for variation of thermal and mechanical properties with age of concrete. Journal of Hydraulic Engineering,42(01):1-7. DOI:10.13243/j.cnki.slxb.2011.01.014.
- [9] Zhu B F.(2012) The thermal control and thermal stress of mass concrete (second edition). China Water&Power Press, BeiJing. www.waterpub.com.cn
- [10] Ministry of Housing and Urban-Rural Development of the People's Republic of China.(2018) GB 50496—2018 Standard for Construction of Mass Concrete. Beijing: China Architecture and Building Press, (in Chinese). https://www.mohurd.gov.cn/gongkai/zhengce/zhengcefilelib/201805/20180511_246272.html
- [11] Ministry of Housing and Urban-Rural Development of the People's Republic of China. (2017)GB50176—2016 Thermal design code for civil building. Beijing:China: Architecture and Building Press, (in Chinese). https://www.mohurd.gov.cn/gongkai/zhengce/zhengcefilelib/201702/20170214_230579.html
- [12] Ma C C, Li S Y, Zhao L J, Liu C Y. (2012)Research on the calculation method of superficial heat preservation of massive concrete structure. Journal of Northwest A & F University(Natural Science Edition), 40(06):217-223. DOI:10.13207/j.cnki.jnwafu.2012.06.008
- [13] Li L, Xiao H, Cheng B W, etc.(2016) Testing of thermal conductivity of fiber based on transient plane heat source method. Journal of Textile Research,37(12):18-23. DOI:10.13475/j.fxb.20160203606
- [14] Schindler K A .Effect of Temperature on Hydration of Cementitious Materials[J].Materials Journal,2004,101(1).DOI:10.1109/ICMENS.2004.150904
- [15] Zhang Z Q, Shi M X, Wang Q, Cui Q.(2016)Accuracy of equivalent age method for predicting mass concrete properties. Journal of Tsinghua University(Science and Technology) ,56(08):806-810. DOI:10.16511/j.cnki.qhdxxb.2016.25.018
- [16] Y Hansen P F,Pedersen E J.Maturity computer for controlled curing and hardening of concrete strength [J].Nordisk Betong,1977,1(19):19-34. <http://worldcat.org/issn/0029130700291307>
- [17] Lee, Yun, Kim, Jin-Keun. Numerical analysis of the early age behavior of concrete structures with a hydration based microplane model[J]. COMPUTERS & STRUCTURES, 2009, 87(17-18): 1085-1101. DOI:10.1016/j.compstruc.2009.05.008.
- [18] Cui W, Chen W, Wang N.(2014)Early Concrete Thermal Parameters Optimization and Accurate Thermal Field Simulation [J]. Advanced Engineering Sciences, 46(03):161-167. DOI:10.15961/j.jsuese.2014.03.008.
- [19] Chen H, Deng G, Zhang Y Y, etc.(2021)Simulation of faced rockfill dams considering temperature change and long-term deformation. Journal of Hydroelectric Engineering, 40(10):124-134. DOI:10.11660/slfjdx.20211012